Inorganic Chemistry

ARTICLE

pubs.acs.org/IC

Investigation Relevant to the Conformation of the 17-Membered Pt(d(GpG)) Macrocyclic Ring Formed by Pt Anticancer Drugs with DNA: Pt Complexes with a Goldilocks Carrier Ligand

Vidhi Maheshwari, Patricia A. Marzilli, and Luigi G. Marzilli*

Department of Chemistry, Louisiana State University, Baton Rouge, Louisiana 70803, United States

Supporting Information

ABSTRACT: Platinum anticancer drug DNA intrastrand cross-link models, LPt(d(G*pG*)) (G* = N7-platinated G residue, L = R_4dt = bis-3,3′-(5,6-dialkyl)-1,2,4-triazine), and R = Me or Et), undergo slow Pt−N7 bond rotation. NMR evidence indicated four conformers (HH1, HH2, ΔHT1, and ΛHT2); these have different combinations of guanine base orientation (head-to-head, HH, or head-to-tail, HT) and sugar−phosphodiester backbone propagation relative to the 5′-G* (the same, 1, or opposite, 2, to the direction in B DNA). In previous work on LPt(d(G*pG*)) adducts, Pt−N7 rotation was too rapid to resolve conformers (small L with bulk similar to that in active drugs) or L was too bulky, allowing formation of only two or three conformers; ΛHT2 was not observed under normal conditions. The (R_4dt)Pt(d(G*pG*)) results support our initial hypothesis that R_4dt ligands have Goldilocks bulk, sufficient to slow G* rotation but insufficient to prevent formation of the ΛHT2 conformer. Unlike the (R_4dt)Pt(5′-GMP)$_2$ adducts, ROESY spectra of (R_4dt)Pt(d(G*pG*)) adducts showed no EXSY peaks, a result providing clear evidence that the sugar−phosphodiester backbone slows conformer interchange. Indeed, the ΛHT2 conformer formed and converted to other conformers slowly. Bulkier L (Et_4dt versus Me_4dt) decreased the abundance of the ΛHT2 conformer, supporting our initial hypothesis that steric crowding disfavors this conformer. The (R_4dt)Pt(d(G*pG*)) adducts have a low abundance of the ΔHT1 conformer, consistent with the proposal that the ΔHT1 conformer has an energetically unfavorable phosphodiester backbone conformation; its high abundance when L is bulky is attributed to a small d(G*pG*) spatial footprint for the ΔHT1 conformer. Despite the Goldilocks size of the R_4dt ligands, the bases in the (R_4dt)Pt(d(G*pG*)) adducts have a low degree of canting, suggesting that the ligand NH groups characteristic of active drugs may facilitate canting, an important aspect of DNA distortions induced by active drugs.

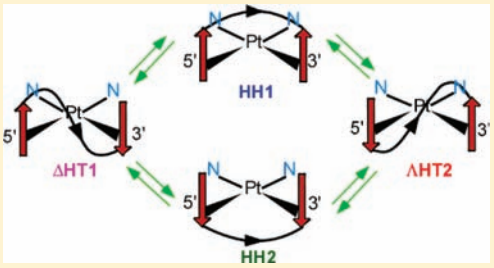

INTRODUCTION

Cisplatin (*cis*-Pt(NH$_3$)$_2$Cl$_2$) and related LPtX$_2$ analogues (L = one bidentate or two *cis*-unidentate N-donor ligands, X$_2$ = anionic leaving ligands) have long enjoyed expanding clinical use in the fight against cancer.[1−5] Pt(II) compounds with trans leaving groups, only one leaving group, or even no leaving group have shown promising activity; these compounds may have different mechanisms of action, different transporters into cells, or activity against different cancers when compared to cisplatin.[2−4,6−19]

An intrastrand DNA cross-link with Pt linking N7's of adjacent guanines of DNA, LPt(d(G*pG*)) (G* = N7-platinated G residue linked by a sugar−phosphodiester backbone), is thought to be the critical lesion accounting for activity for such cis-bifunctional Pt(II) compounds.[20−22] Here, d(G*pG*) is used to indicate the cross-link dinucleotide moiety in DNA, in an oligonucleotide strand, or within an LPt(d(G*pG*)) adduct of the dinucleotide. The L ligands in the cis-active agents (such as the very successful clinical agent oxaliplatin [(1*R*,2*R*-diaminocyclohexane)oxalatoplatinum(II)])[20,23,24] have relatively low bulk in the vicinity of the two G*'s. When L is bulky, activity decreases and toxicity increases.[3,20,25−28] However, recent results suggest that the opposite situation may hold true for monofunctional Pt(II) agents, for which greater bulk in ligands appears to be correlated with enhanced activity.[8,29,30] In our view, bulk is also important for activity of trans-bifunctional Pt(II) compounds.[31−35] Platinum agents with leaving groups all preferentially attack guanine in DNA. For these various classes of compounds, understanding the effect of carrier-ligand bulk on DNA distortions, on activity, on mechanism of action, and on toxicity is obviously an essential aspect of designing new drugs.[36] One aspect of such distortions relates to base canting. In active drugs, one guanine base in adducts is not perpendicular to the coordination plane but is highly canted, and the DNA distortion is intimately linked to the canting.[36−39]

The effect of bulk of the nonleaving ligand in both mono- and bifunctional Pt(II) agents can be classified into three categories as follows: on the dG* or d(G*pG*) unit, on the nearby DNA sequence, and on the contacts that proteins or enzymes can make with the adduct. These effects are expected to be mutually interdependent. For example, evidence is mounting for the importance of a very distorted base pair (bp) step, which we refer to as the Lippard bp step, adjacent to the d(G*pG*) cross-link in

Received: March 11, 2011
Published: June 13, 2011

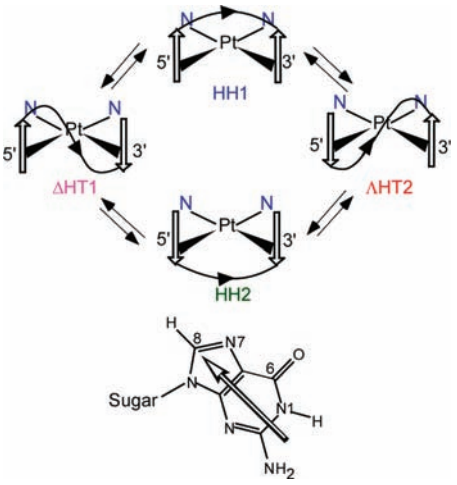

Figure 1. Depiction of the four conceivable combinations of two possible base orientations and two possible sugar−phosphate backbone propagation directions for d(G*pG*).[22,39,44,52] G* coordination sites are forward, and the Pt and carrier ligand (not shown except for N-donor atoms) are to the rear. The unfilled arrows represent the G* base (shown below the scheme). The arrowhead denotes the G* H8. Base canting is not illustrated. The two base orientations are head-to-head (HH) and head-to-tail (HT). The filled arrowheads in the curved lines connecting the G* base arrows indicate the 5′-G* to 3′-G* direction of propagation of the sugar−phosphodiester backbone; this direction of propagation from 5′ to 3′ along the backbone is clockwise in HH1 and ΔHT1 and is counterclockwise in HH2 and ΛHT2. These designations are color coded, and where possible, this coding is adopted in subsequent figures. The small straight arrows indicate how the conformers are related by a single base rotation about the Pt−N7(G*) bond and are not meant to describe the relation of the backbone to the base (i.e., the anti or syn conformation of the G* residue) or the reaction pathways, which are discussed briefly in the Supporting Information.

the 5′ direction.[21,40,41] Possibly this DNA distortion near the cross-link is needed to accommodate the Pt−NH_3 group cis to the 5′-G*; the steric effect of this relatively small Pt−NH_3 group appears to be magnified by the cross-link structure,[30] which, as mentioned, has a canted base.[36−38,42−45] We believe that canting is a key structural feature that places the ligand close to the base pair adjacent to the cross-link.[36−38,42−45]

In the d(G*pG*) cross-link, the bases can have a head-to-head (HH) or a head-to-tail (HT) orientation and the HT orientation has intrinsic chirality, labeled as Δ and Λ (see Figure 1). The sugar−phosphodiester backbone can have the direction of propagation relative to the 5′-G* either the same as (labeled 1) or opposite to (labeled 2) that of B DNA (Figure 1).[22,36,37,42,44,46−53] The combination of these two structural features gives rise to four conformers (Figure 1). Other conformational features of the conformers are the G* sugar pucker and the syn or anti conformation of each G* residue. Thus, several subconformers within these four conformer classes can be imagined. The commonly observed HH1 conformer has both residues anti, and the sugar pucker is N for 5′-G* and S for 3′-G*.[21,22,30,36,41,42,44,51−54]

In simple LPt**G**$_2$ adducts, which lack a phosphodiester backbone (boldface **G** indicates a guanine derivative not linked to another nucleoside by a backbone), HT conformers are favored.[39,55−59] In contrast, the cross-link is generally accepted to favor the HH1 conformation in both duplexes and single strands.[39] In the absence of an X-ray structure for *cis*-Pt(NH_3)$_2$(d(G*pG*)), the simplest cross-link adduct, the observation of only one set of ^{1}H

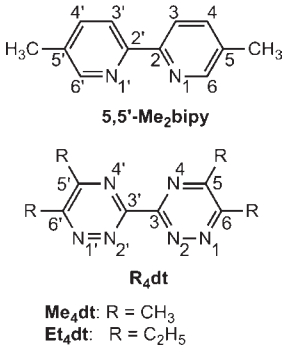

Figure 2. Numbering scheme for 5,5′-dimethylbipyridine (5,5′-Me_2bipy) and bis-3,3′-(5,6-dialkyl-1,2,4-triazine) (R_4dt) ligands.

NMR signals can be taken to imply that the presence of the backbone favors the HH base orientation over the otherwise favored HT orientation.[37,44,47,52] Alternatively, multiple conformers of *cis*-Pt(NH_3)$_2$(d(G*pG*)) could be present, but fast interchange between conformers time averages the signals, explaining the presence of one set of signals.[39] We refer to these conflicting interpretations of NMR data as the 'fast dynamic motion problem'.[22,39,42,44,52,53] To overcome this problem, we employed LPt(d(G*pG*)) with bulky L designed to reduce the rate of dynamic motion by approximately a billion-fold as compared to that of *cis*-Pt(NH_3)$_2$(d(G*pG*)).[22,58−60] These studies initially employed moderately bulky L.[22,43,44,53] However, a very recent study of LPt(d(G*pG*)) adducts employed very large *N,N,N′,N′*-tetramethyldiamine carrier ligands.[36] All such studies have shown that an abundant HH1 conformer is always present in an equilibrium mixture with one or both of the HH2 and ΔHT1 conformers (Figure 1).[22,36,42,44,52,53]

As mentioned above, in addition to the four overall conformers of the large 17-membered macrocyclic ring in LPt(d(G*pG*)) adducts, several other conformers differing in sugar pucker or nucleotide conformation (i.e., the anti or syn conformation of the G* residue) could be envisioned. The ΛHT2 conformer was not observed when the d(G*pG*) unit is in its normal protonation state with both G*'s having N1H groups. The lack of an obvious explanation for the low stability of the ΛHT2 and other conformers indicates that our understanding of the factors influencing the conformation of the 17-membered Pt(d(G*pG*)) macrocyclic ring is incomplete. Another unresolved issue is the relationship of canting to carrier-ligand properties; one such property is the presence of NH groups, which could be responsible for canting by forming hydrogen bonds with the guanine base O6 group (Figure 1).[61] The relationship of canting to the Pt-induced DNA distortion and anticancer activity was mentioned above.

To address some of the issues that remain from studies employing highly dynamic adducts with small carrier ligands or using nondynamic adducts with moderately to very bulky carrier ligands, our goal became to identify a ligand with Goldilocks-type bulk near the guanine coordination sites, i.e., bulk large enough to slow dynamic motion but not so large as to prevent canting or to destabilize the ΛHT2 conformer. Recently, we discovered that (R_4dt)Pt(5′-GMP)$_2$ adducts (R_4dt = bis-3,3′-(5,6-dialkyl-1,2,4-triazine), Figure 2) have a high abundance of the HH conformer.[57] The overall low steric effects of the R_4dt ligands (R = Me, Et), with two N + N lone pair groupings, allow enough space for the HH conformer to exist without significant clashes between the O6 atoms of the 5′-GMP's.[57] However, R_4dt ligands

dx.doi.org/10.1021/ic200512m |*Inorg. Chem.* 2011, 50, 6626–6636

possess enough bulk to reduce the Pt−N7(**G**) rotation rate. Thus, we evaluate here both the distribution and the characteristics of conformers formed by the $(Me_4dt)Pt(d(G^*pG^*))$ and $(Et_4dt)Pt(d(G^*pG^*))$ adducts (Figures 1 and 2). Finally, the results for these adducts and previous results for $(R_4dt)Pt(5'\text{-GMP})_2$ adducts have allowed us to assess a key uncertainty involving the backbone in the cross-link, namely, whether or not the backbone reduces the interchange rates between conformers of an $LPt(d(G^*pG^*))$ adduct versus the rates of the corresponding $LPt\mathbf{G}_2$ adduct. In order to make direct comparisons with previous studies using planar bidentate aromatic ligands,[22,53,57] we used D_2O/DMSO-d_6 solutions. Dissolution of the starting $(R_4dt)PtCl_2$ complex in DMSO-d_6 bypasses the need to convert the complex to the diaqua derivative.

EXPERIMENTAL SECTION

Starting Materials. 2′-Deoxyguanyl(3′→5′)-2′-deoxyguanosine (d(GpG)) was used as received from Sigma. Syntheses of the R_4dt complexes (Figure 2), $(Me_4dt)PtCl_2$ (Me_4dt = bis-3,3′-(5,6-dimethyl-1,2,4-triazine)) and $(Et_4dt)PtCl_2$ (Et_4dt = bis-3,3′-(5,6-diethyl-1,2,4-triazine)), have been described elsewhere.[57]

Reaction of $(R_4dt)PtCl_2$ with d(GpG). Because of the low solubility of $(R_4dt)PtCl_2$ in D_2O, solutions containing an equimolar ratio of Pt:d(GpG) were prepared by mixing a DMSO-d_6 solution of $(Me_4dt)PtCl_2$ (1.32 mg/200 μL, 5 mM) or $(Et_4dt)PtCl_2$ (2.07 mg/400 μL, 7 mM) with a D_2O solution of d(GpG) (1.70 mg/350 μL or 2.38 mg/150 μL, respectively). (Less DMSO-d_6 was needed for $(Me_4dt)PtCl_2$, which is more soluble than $(Et_4dt)PtCl_2$ in D_2O.) The D_2O:DMSO-d_6 reaction mixture was 64:36 by volume when R = Me and 27:73 by volume when R = Et. The solutions were maintained at pH 4.0 and 5 °C and carefully monitored for 2 days by ^{1}H NMR spectroscopy until no free d(GpG) signals were observed. DNO_3 and NaOD solutions (0.1 M in D_2O) were used to adjust the pH of D_2O/DMSO-d_6 solutions. For comparison, 275 μL of the $(Et_4dt)Pt(d(G^*pG^*))$ solution was diluted to 3.5 mM with 275 μL of D_2O to obtain the same 64:36 D_2O:DMSO-d_6 mixture as that used for $(Me_4dt)Pt(d(G^*pG^*))$. The $(R_4dt)Pt(d(G^*pG^*))$ solutions were monitored by ^{1}H NMR spectroscopy every 24 h for the initial 6 days and then weekly up to 4 months until no change in the H8 signal intensity was observed.

NMR Measurements. ^{1}H NMR spectra were recorded on a Bruker (400 MHz) or a Varian spectrometer (700 MHz) and referenced to the residual HOD signal, assigned a value of 4.78 ppm. A presaturation pulse to suppress the water peak was used when necessary. ^{31}P NMR spectra were referenced to external trimethyl phosphate (0 ppm) in a 64:36 mixture of D_2O:DMSO-d_6. NMR data were processed with XWINNMR or Mestre-C software.

Matrices (512 × 1024 and 512 × 2048) were collected for ^{1}H−^{1}H COSY and (500 and 600 ms delay) ROESY experiments on the 400 MHz Bruker spectrometer and 700 MHz Varian spectrometer, respectively; both experiments were conducted at 25 °C with a spectral window of ∼6000 and ∼8000 Hz on 400 and 700 MHz spectrometers, respectively. A presaturation pulse of ∼1 s was used to reduce the HOD signal. Typically, 32 scans were collected per block. An exponential apodization function with a line broadening of 0.2 Hz and a phase-shifted 90° sine bell function were used to process the ROESY t_2 and t_1 data, respectively.

Circular Dichroism (CD) Spectroscopy. All samples used for CD experiments were prepared from the respective NMR samples by diluting to ∼0.025 mM Pt with deionized water. The concentration of the CD samples was determined by measuring the absorption at 260 nm on a UV−vis spectrometer (d(GpG) ε_{260} = 21.6 mM^{-1} cm^{-1}). Spectra were recorded from 400 to 200 nm at a scan speed of 50 nm/min on a JASCO J-600 CD spectropolarimeter. Six scans were recorded and averaged for each sample.

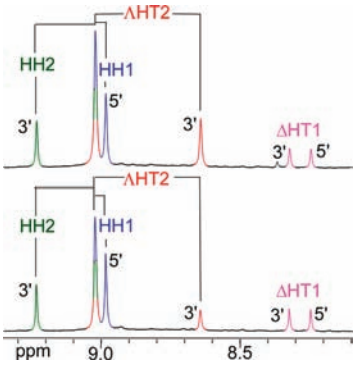

Figure 3. ^{1}H NMR spectra (400 MHz) in the H8 region for $(Me_4dt)Pt(d(G^*pG^*))$ collected at room temperature after 1 week (bottom) and after 8 weeks (top) (pH 4.0, in D_2O/DMSO-d_6). The H8 signals for the various conformers are labeled and color coded.

High-Performance Liquid Chromatography (HPLC). Chromatograms were obtained on a Varian ProStar HPLC instrument with a PDA detector operating at 254 nm. Separations employed a Microsorb 100-5 C8 150 × 4.6 mm reverse-phase column. Eluants A and B both contained 0.02 M ammonium acetate buffer, pH 5.5. Solvent A was water, and solvent B was a 2:1 methanol:water mixture. A flow rate of 0.70 mL/min was maintained over the course of a 40 min linear gradient (0 min = 95% A and 5% B, 40 min = 48% A and 52% B) for the $(R_4dt)Pt(d(G^*pG^*))$ adducts. The NMR sample was diluted to obtain a 1.7 mM solution. Each eluted fraction was collected, concentrated to a small volume (200 μL), and stored at 25 °C to see if equilibration occurred. A 20 μL sample of each fraction was reinjected after 2 h and then after intervals of 24 h for 7 days and finally at weekly intervals for 2 months. The percentage of each product separated by HPLC was measured by integration of the corresponding peak area.

RESULTS

Conformer Assignment and Conformational Features. For the $(R_4dt)Pt(d(G^*pG^*))$ adducts, ^{1}H−^{1}H ROESY and COSY data were used to assign H8 and sugar proton signals. Structural features of conformers were assessed by standard methods. The S- and N-sugar pucker conformations were identified from the characteristic H1′ coupling patterns and the existence of H8−H3′ NOE cross-peaks for N-sugars.[22,53] The G* nucleotide conformations can be assessed by strong intraresidue H8−H2′/H2″ NOE cross-peaks and weak (or unobservable) H8−H1′ cross-peaks for the anti conformation and stronger H8−H1′ NOE cross-peaks for the syn conformation.[22,53] Because the G* H8 atoms are closer to each other in the HH conformers than in the HT conformers, the observation of an H8−H8 NOE cross-peak is indicative of an HH conformer, whereas the absence of such a cross-peak is characteristic of an HT conformer.[52] When compared to free d(GpG), HH and ΔHT1 conformers of $LPt(d(G^*pG^*))$ complexes often show characteristic NMR shift changes; more downfield H8 and ^{31}P signals indicate HH conformers,[47,62−64] whereas slightly shifted H8 and more upfield ^{31}P NMR signals indicate a ΔHT1 conformer.[42,52]

$(Me_4dt)Pt(d(G^*pG^*))$. In 64:36 D_2O:DMSO-d_6 solution at pH ≈ 4.0 and 5 °C, the $(Me_4dt)Pt(d(G^*pG^*))$ adduct was formed rapidly and completely within ∼30 min of mixing $(Me_4dt)PtCl_2$ in a 1:1 molar ratio with d(GpG) (H8 signals at 8.06 and 7.83 ppm).

dx.doi.org/10.1021/ic200512m |*Inorg. Chem.* 2011, 50, 6626–6636

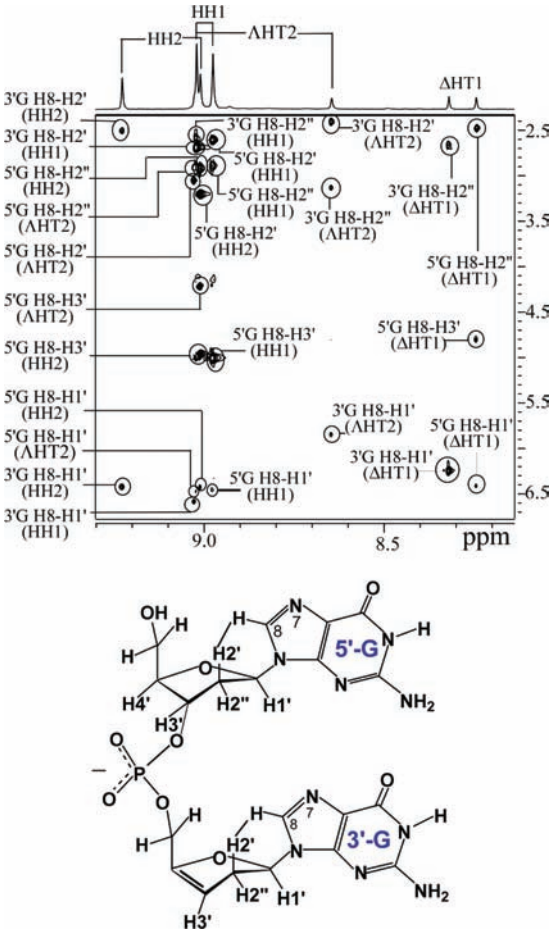

Figure 4. NOE cross-peaks from the G* H8 signals to deoxyribose signals (H1′, H2′, H2″, and H3′) in a ^{1}H−^{1}H ROESY spectrum (700 MHz, 600 ms mixing time) of a 1-week-old (Me_4dt)Pt(d(G*pG*)) sample at pH 4.0 and 25 °C.

This rapid reaction was repeated several times with similar results, consistent with rapid formation of four conformers (Figures 3, 4, S2, Supporting Information, and S3, Supporting Information). The resolution of new peaks in the crowded region near 9 ppm varied somewhat from mixed-solvent sample to sample, with clearly resolved nonoverlapped peaks rarely observed. (Figure S2, Supporting Information, has eight peak tops resolved.) The intensity of these new peaks establishes that some samples contain overlapping G* H8 signals; at 400 MHz, the peak at 9.03 ppm - (Figure 3) contains three overlapped G* H8 signals. This peak in this sample was slightly better resolved at 700 MHz to give two distinct G* H8 peaks at 9.03 and 9.02 ppm; ROESY data (Figure 4) establish that the 9.03 ppm peak contains two overlapping G* H8 signals, even at 700 MHz. H8−H8 NOE cross-peaks (from one 9.03 ppm signal to the 8.98 ppm signal and from the 9.02 ppm signal to the 9.23 ppm signal, not shown) allow us to attribute these H8 signals to HH conformers.

For the more abundant HH conformer (H8 signals at 9.03 and 8.98 ppm), the G* H8−H2′/H2″ cross-peaks were stronger than the H8−H1′ cross-peaks (Figure 4), consistent with a predominantly anti conformation for both G* residues. The NOE cross-peak from the H8 signal at 8.98 ppm to an H3′ signal (Figure 4) characteristic of an N-sugar pucker allows assignment of this H8 signal to the 5′-G* residue, which typically has an N-pucker in

Table 1. ^{1}H and ^{31}P NMR Signal Assignments (ppm) for (R_4dt)Pt(d(G*pG*)) Adducts (pH ≈ 4, 25 °C)[a]

L	conformer	G*	H8	H1′	H2′	H2″	H3′	H4′	residue[a]	^{31}P
Me_4dt	HH1	5′	8.98	6.44	2.60	2.89	5.00	4.16	anti	−3.43
		3′	9.03	6.46	2.69	2.60	4.70	4.25	anti	
Et_4dt	HH1	5′	9.04	6.39	2.55	2.80	4.92	4.08	anti	−3.41
		3′	8.97	6.43	2.61	2.53	4.64	4.22	anti	
Me_4dt	HH2	5′	9.02	6.42	3.19	2.91	4.96	4.14	anti	−2.76
		3′	9.23	6.40	2.51	2.82	4.74	4.50	anti	
Et_4dt	HH2	5′	9.10	6.37	3.15	2.88	5.01	4.08	anti	−2.51
		3′	9.23	6.32	2.32	2.72	4.65	4.41	anti	
Me_4dt	ΔHT1	5′	8.24	6.40	3.22	2.49	4.74	4.19	anti	−5.01
		3′	8.31	6.24	3.48	2.66	4.81	4.12	syn	
Et_4dt	ΔHT1	5′	8.32	6.35	3.52	2.65	4.76	4.02	anti	−4.72
		3′	8.29	6.19	3.35	2.61	4.88	4.10	syn	
Me_4dt	ΛHT2	5′	9.03	6.57	3.04	2.90	4.13	4.99	anti	−4.09
		3′	8.65	5.84	2.40	2.84	4.83	4.69	anti	
Et_4dt	ΛHT2	5′	8.99	6.50	2.82	2.78	4.59	[b]	anti	−4.01
		3′	8.66	5.98	2.39	2.72	[b]	[b]	anti	

[a] Conformational assignment (anti/syn) based on the relative strength of NOE cross-peaks between H8 resonances and H1′ or H2′/H2″ signals in the ROESY spectrum. [b] Signals not detected.

such cross-links.[21,44,52,53,64] The H8 signal at 9.03 ppm, which must be the 3′-G* H8 signal, has no H8−H3′ cross-peak, consistent with the expected S-sugar pucker for the 3′-G* residue.

For the less abundant HH conformer of the (Me_4dt)Pt(d(G*pG*)) adduct, the strong H8−H3′ cross-peak indicates that the G* H8 signal at 9.02 ppm belongs to the 5′-G*, with an N-sugar pucker; the H8 signal at 9.23 ppm has no H8−H3′ NOE cross-peak, indicating a 3′-G* S-sugar pucker (Figure 4). The observation of stronger 5′-G* H8−H2′/H2″ cross-peaks than the H8−H1′ cross-peak is consistent with an anti conformation.[22,37,46,52,53] For the 3′-G*, weak H8−H2′ and H8−H1′ NOE cross-peaks were observed (Figure 4). Thus, both HH conformers adopt an anti,anti conformation. The H8-sugar proton distances in molecular mechanics/dynamics computations on the HH conformers of (Me_2ppz)Pt(d(G*pG*)) (Me_2ppz = *N*,*N*′-dimethylpiperazine) are too long for observable H8−sugar NOE's for the 3′-G* residue of the HH2 conformer.[53] The observation of weak 3′-G* H8-to-sugar cross-peaks for the less abundant HH conformer and strong 3′-G* H8-to-sugar cross-peaks for the more abundant HH conformer led us to assign these as the HH2 and HH1 conformers, respectively. (Assignments for signals of all conformers are presented in Table 1.) These ^{1}H NMR shifts and ^{31}P NMR shifts (see below) are consistent with those for the HH2 and HH1 conformers of (*R*,*S*,*S*,*R*)-BipPt(d(G*pG*))[44] (Bip = 2,2′-bipiperidine) and (Me_2ppz)Pt(d(G*pG*)).[53]

For the (Me_4dt)Pt(d(G*pG*)) adduct, there are also two other pairs of H8 signals at 8.31 and 8.24 ppm and at 8.65 ppm and within the 9.03 ppm peak. Neither pair showed H8−H8 NOE cross-peaks in the ROESY spectra collected for both the 1-week-old and the 3-month-old samples of (Me_4dt)Pt(d(G*pG*)).

Because of the absence of an H8−H8 NOE and the upfield ^{31}P NMR shift (two features characteristic of the ΔHT1 conformer),[22,42,44,52] the H8 signals at 8.31 and 8.24 ppm and the ^{31}P NMR signal at −5.01 ppm were assigned to the ΔHT1 conformer (Table 1). This upfield ^{31}P NMR shift is consistent

dx.doi.org/10.1021/ic200512m |*Inorg. Chem.* 2011, 50, 6626–6636

Table 2. Equilibrium Conformer Distribution (%) for LPt(d(G*pG*)) Adducts When L Lacks NH Groups

L	HH1	HH2	ΔHT1	ΛHT2
Me_4dt	36	18	6	40
Et_4dt	41	33	9	17
Me_2ppz[a]	50	20	30	
5,5-Me_4bipy[b]	54	11	35	
(*R*,*R*)-Me_4DAB[c]	54	8	38	
(*S*,*S*)-Me_4DAB[c]	34		66	

[a] Reference 53. [b] Reference 22. [c] Reference 36.

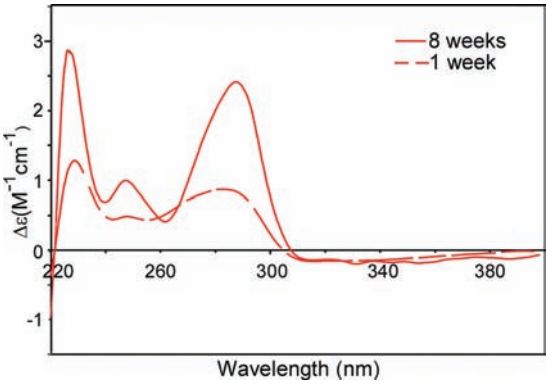

Figure 5. CD spectra of a (Me_4dt)Pt(d(G*pG*)) sample recorded in water at pH ≈ 4 and 25 °C. The positive feature at ~290 nm is indicative of a ΛHT conformation.

with those of the ΔHT1 conformer of both (5,5′-Me_2bipy)Pt(d(G*pG*)) (−4.74 ppm, 5,5′-Me_2bipy = 5,5′-dimethylbipyridine, Figure 2) and (Me_2ppz)Pt(d(G*pG*)) (−5.12 ppm).[22,53] For the (Me_4dt)Pt(d(G*pG*)) ΔHT1 conformer, the G* H8 signal at 8.24 ppm exhibits an intraresidue H8−H3′ NOE cross-peak (Figure 4) consistent with a 5′-G* N-sugar pucker. A strong 5′-G* H8−H2″ cross-peak and a weak H8−H1′ cross-peak indicate an anti 5′-G* conformation. For the H8 signal at 8.31 ppm, the absence of an H8−H3′ NOE and the observation of a doublet of doublets coupling pattern for the H1′ signal (6.24 ppm) are indicative of a 3′-G* S-sugar pucker. Strong 3′-G* H8−H1′ NOE and weak H8−H2″ cross-peaks indicate a syn 3′-G* conformation. Thus, the ΔHT1 conformer adopts an anti,syn conformation, as has been found previously.[22,42,52,53]

The three pairs of H8 signals discussed thus far are fully consistent with the formation of HH1, HH2, and ΔHT1 conformers, as observed for all other LPt(d(G*pG*)) adducts.[22,53] However, a significant fourth pair of H8 signals (at 8.65 and 9.03 ppm) present at low pH (<8) is unprecedented. Moreover, the intensity increased slowly over a period of ~3 months, until finally this pair had the highest intensity of the four pairs. Because it exhibits no H8−H8 NOE cross-peak, this kinetically disfavored but thermodynamically favored conformer has features most consistent with an HT conformer, such as the ΛHT2 conformer. The distribution of the HH1, HH2, ΔHT1, and (likely) ΛHT2 conformers changed from 42%, 37%, 11%, and 10% (after 1 week) to 36%, 18%, 6%, and 40% (after ~3 months), respectively (Table 2 and Figure S2, Supporting Information). Because HH conformers have no intrinsic chirality arising from the orientation of the bases, the CD signal shape has proved to be a definitive means for assigning the chirality of the

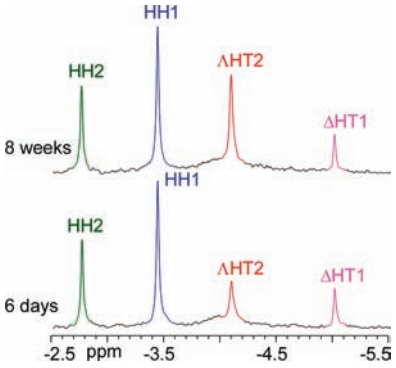

Figure 6. ^{31}P NMR spectrum (400 MHz) of (Me_4dt)Pt(d(G*pG*)) after 6 days (bottom) and after 8 weeks (top) in D_2O/DMSO-d_6 at pH 4.0 and 25 °C. The assignments are color coded. Note that the stack plot keeps the HH1 signal height the same because it is the highest signal. The ΛHT2 conformer grows slowly and as mentioned in the text does not interchange with the other conformers nearly as fast as the others interchange with each other. Thus, the ratio of ΔHT1, HH1, and HH2 peak heights remain the same, while the total abundance of these conformers decreases with time. This result follows directly from our conclusions.

major HT conformer when that HT conformer clearly dominates.[53] A (Me_4dt)Pt(d(G*pG*)) sample at 8 weeks (HH1, HH2, ΔHT1, and (likely) ΛHT2 distribution = 40%, 25%, 10%, and 25%) gave a positive CD feature at ~290 nm (Figure 5) characteristic of the ΛHT conformer of LPt**G**$_2$ adducts.[42,60,65,66] This feature is consistent with the assignment of the slowly forming species as the elusive ΛHT2 conformer. Other shorter wavelength CD features also aid in assignment of conformation,[67] but the ditriazine ligand absorbs in the UV region, limiting the use of CD spectroscopy in the present case.

For the (Me_4dt)Pt(d(G*pG*)) ΛHT2 conformer, the G* H8 signals at 8.65 and 9.03 ppm have H8−H2′/H2″ cross-peaks stronger than the H8−H1′ cross-peak (Figure 4), indicating an anti conformation for both G* residues. The H8−H3′ NOE cross-peak (9.03−4.13 ppm) and an H1′ doublet for this residue are both consistent with a 5′-G* N-sugar pucker. The absence of an observable H8−H3′ cross-peak (8.65−4.83 ppm) and the doublet of doublets coupling pattern for the H1′ signal indicate a 3′-G* S-sugar pucker.

The distribution of ^{1}H NMR signal intensities continued to change for 8−12 weeks and did not change thereafter. The final distribution of conformers of (Me_4dt)Pt(d(G*pG*)) at equilibrium determined by these intensities is shown in Table 2, where the distribution is compared to that for other LPt(d(G*pG*)) adducts lacking NH groups.

^{31}P NMR Spectroscopy. Compared to the −4.20 ppm value of the unstrained d(GpG) phosphodiester group measured in this solvent mixture, the ^{31}P NMR signals of the HH conformers are downfield and the signal for the ΔHT1 conformer is upfield. From their relative intensities, ^{31}P NMR signals at −2.76, −3.43, and −5.01 ppm for the (Me_4dt)Pt(d(G*pG*)) adduct (Figure 6) were, respectively, assigned to the HH2, HH1, and ΔHT1 conformers on the basis of the intensity and close similarity to the shifts for other LPt(d(G*pG*)) adducts.[22,53] In addition, a fourth peak at −4.09 ppm slowly increased with time, indicating that this signal belongs to the ΛHT2 conformer, which slowly increases in abundance with time.

Slow Conformer Interchange Rates. Consistent with the long times needed for the NMR signals to redistribute, EXSY

dx.doi.org/10.1021/ic200512m |*Inorg. Chem.* 2011, 50, 6626–6636

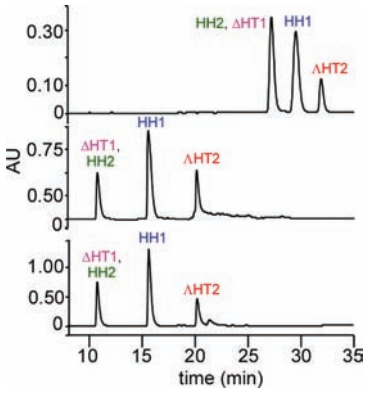

Figure 7. HPLC chromatograms of a 1-week-old $(Me_4dt)Pt(d(G^*pG^*))$ sample (bottom), an 8-week-old $(Me_4dt)Pt(d(G^*pG^*))$ sample (middle), and a 1-week-old $(Et_4dt)Pt(d(G^*pG^*))$ sample (top).

Table 3. Conformer Distribution (%) for LPt(d(G*pG*)) Adducts after 1 Week of Reaction Time[a]

L	HH1	HH2 + ΔHT1	ΛHT2
Me_4dt	52 (15.7)	28 (10.8)	20 (20.3)
Et_4dt	44 (29.5)	42 (27.2)	14 (31.9)

[a] Distribution determined by HPLC, with retention times (min) given in parentheses.

cross-peaks were absent in the ROESY spectrum of the $(Me_4dt)Pt(d(G^*pG^*))$ adduct. These results indicate that the rate of interconversion between the conformers in $(Me_4dt)Pt(d(G^*pG^*))$, an adduct with bases linked by the sugar−phosphodiester backbone, is considerably slower than that for rotamers of $(Me_4dt)Pt(GMP)_2$, adducts with unlinked **G** derivatives.[57] This slow rate for the $(Me_4dt)Pt(d(G^*pG^*))$ adduct allowed the separation of the conformers by HPLC.

HPLC Analysis of $(Me_4dt)Pt(d(G^*pG^*))$. When a 1-week-old NMR sample of the $(Me_4dt)Pt(d(G^*pG^*))$ adduct with four conformers was injected, three HPLC peaks were observed with retention times (RT) of 10.8, 15.7, and 20.3 min in 28%, 52%, and 20% abundance, respectively (Figure 7 and Table 3). Because the NMR data for this sample reveal that the HH1 conformer is most abundant, the largest peak (RT = 15.7 min) contains the HH1 conformer. The intensity of the peak at RT = 20.3 min increased with time (Figure 7), indicating that this fraction contains the ΛHT2 conformer. Thus, the 10.8 min fraction contains two conformers, ΔHT1 and HH2.

A 1.7 mM sample of $(Me_4dt)Pt(d(G^*pG^*))$ for HPLC analysis was prepared by diluting an aliquot of the NMR sample (7 mM) with water. At least three 20 μL injections of this dilute sample were made in order to collect a sufficient amount of each fraction for reinjections. Because the concentration of each collected fraction was low (combined volume, 1−3 mL), the volume was reduced under vacuum. The residual liquid (containing ammonium acetate) was taken up in water to give a final volume of ~200 μL. This procedure provided sufficient sample for injections at several different time intervals. The intensity of the peaks in the HPLC traces changed with time as the conformer distribution changed. Because the peaks in the initial separation of the diluted NMR sample varied from 20% to 52%, the total Pt concentration in each re-equilibrating sample varied from 0.10 to 0.27 mM; these values are much lower than the starting 1.7 mM value because the total volume of the three re-equilibrating samples was 600 μL, about 10 times the total volume for the initial injections. At various time intervals, an aliquot of each sample was reinjected. Each aliquot when reinjected gave a chromatogram with four peaks (RT = 11.3, 12.2, 16.0, and 20.9 min) (Supporting Information, Figures S4−S6). The small differences from the initial RT values and the improved resolution of the peaks relative to the initial chromatogram are attributed to the presence of ammonium acetate, which was not present in the original NMR samples used for the initial HPLC separations.

HPLC analysis of the reinjected peaks gave evidence that the ΔHT1, HH2, and HH1 conformers interchanged relatively quickly. The change in HPLC peak intensity with time upon reinjection of the $(Me_4dt)Pt(d(G^*pG^*))$ peaks was informative. When reinjected, the peak at 15.7 min (HH1) gave a large 16.0 min peak (HH1), which decreased from 72% after 1 day to 51% after 4 days (Supporting Information, Figure S4). The peak at 11.3 min (ΔHT1) decreased from 16% to 14%, and that at 12.2 min (HH2) increased from 12% to 32%. This pattern is consistent with the HH1 conformer converting to the ΔHT1 conformer, which then converts to the more stable HH2 conformer. Upon reinjection after 1 day, the ΔHT1 + HH2 peak gave peaks for ΔHT1 (42%), HH2 (40%), and HH1 (18%) (Supporting Information, Figure S5). At 4 days the distribution changed to 21% ΔHT1, 30% HH2, and 48% HH1, again consistent with ΔHT1 and HH2 conformers redistributing to the more stable HH1 conformer. Interconversion occurred under dilute conditions (see above). The sample prior to reinjection did not contain any of the initial reactants in the NMR sample. Because the interconversion of these conformers involves only conformational changes of the G* residues, interconversion does not require the presence of the initial reactants and does not depend on concentration. Thus, the types of changes with time observed for the HPLC peaks are consistent with those expected for peaks arising from four interconverting conformers.

Of particular importance, the peaks with the common conformers on reinjection gave evidence for formation of the peak with the long retention time (containing the fourth species). In turn, reinjection of this peak led to the formation of the three well-known conformers. The original 20.3 min fraction (ΛHT2) redistributed very slowly upon reinjection. After 4 days the distribution was 5% ΔHT1, 27% HH2, 9% HH1, and 59% ΛHT2 (Supporting Information, Figure S6). As expected, the ΛHT2 peak (20.9 min) was the largest. However, the ΛHT2 conformer had converted more to the HH2 conformer (12.2 min peak) than to the HH1 conformer (16 min peak). Because the HH1 conformer is more abundant at long times (hence more stable) than the HH2 conformer, the high percentage of the HH2 conformer suggests that the ΛHT2 conformer converts preferentially to the HH2 conformer. Most, if not all, of the HH1 conformer may arise from redistribution of the ΔHT1 conformer (see Supporting Information). These findings provide compelling evidence that all four species are conformers. If the slowest eluting fraction were not from a conformer, it would not so readily convert into known conformers under conditions so different from those employed in the NMR experiments. Thus, the evidence strongly suggests that the fourth species is a fourth conformer.

$(Et_4dt)Pt(d(G^*pG^*))$. Four new pairs of G* H8 NMR signals were observed within minutes after mixing $(Et_4dt)PtCl_2$ and

dx.doi.org/10.1021/ic200512m |*Inorg. Chem.* 2011, 50, 6626–6636

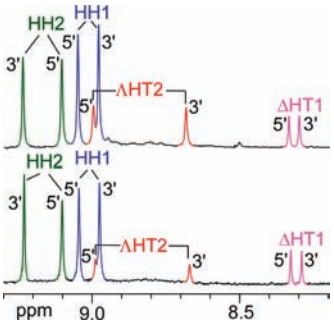

Figure 8. H8 region of the ^{1}H NMR spectrum (400 MHz) of (Et_4dt)Pt(d(G*pG*)) recorded after 1 week (bottom) and after 8 weeks (top) in D_2O/DMSO-d_6 at pH 4.0 and 25 °C. The assignments are color coded.

d(GpG) solutions. After 1 day no free d(GpG) signals were observed, indicating complete reaction. The conformers were characterized by NMR methods as described above, giving overall similar results as found for the (Me_4dt)Pt(d(G*pG*)) adduct but with important differences to be discussed below. Figure 8 illustrates the changes in the NMR signal intensities for the (Et_4dt)Pt(d(G*pG*)) adduct as the conformer distribution changed over time. Details are provided in the Supporting Information, and the NMR properties are summarized in Table 1.

HPLC Analysis of (Et_4dt)Pt(d(G*pG*)). A 1-week-old sample of the (Et_4dt)Pt(d(G*pG*)) adduct gave three HPLC peaks with RT's of 27.2 (42% HH2 + ΔHT1), 29.5 (44% HH1), and 31.9 (14% ΛHT2) min (Figure 7 and Table 3). This three-peak pattern was similar to that for (Me_4dt)Pt(d(G*pG*)), but because of the more hydrophobic ethyl group, the (Et_4dt)Pt(d(G*pG*)) peaks had longer retention times.

As observed for (Me_4dt)Pt(d(G*pG*)), each (Et_4dt)Pt(d(G*pG*)) peak upon reinjection eventually gave four product peaks (RT = 27.7, 28.4, 30.0, and 32.5 min) with retention times influenced by the residual salt and, respectively, attributable to the ΔHT1, HH2, HH1, and ΛHT2 conformers. The conformer redistribution for the (Et_4dt)Pt(d(G*pG*)) adduct upon reinjection of each product peak is discussed in the Supporting Information. For reasons given above, these HPLC observations provide compelling evidence that the four forms detected by NMR spectra must be conformers that re-equilibrate slowly.

The (R_4dt)Pt(d(G*pG*)) ΛHT2 conformer converted to other conformers somewhat faster when R = Et than when R = Me. This finding is consistent with the NMR results, showing that the ΛHT2 conformer is less favored in the (R_4dt)Pt(d(G*pG*)) adduct with the more bulky Et_4dt ligand than in the adduct with the Me_4dt ligand (Table 2).

DISCUSSION

The factors influencing the conformation and the stability of the various possible conformers of the Pt(d(G*pG*)) macrocyclic ring and the dependence of these factors on carrier-ligand properties are intimately tied to the structure of the cross-link and the resulting DNA distortions leading to platinum drug anticancer activity. Our overall goal is to evaluate key incompletely understood aspects of this fundamental chemistry by varying carrier-ligand properties. Published studies on LPt(d(G*pG*)) adducts are best described as having used very small ligands (resulting in rapid conformer interchange) or ligands of moderate bulk. Below, we discuss a recent as yet unpublished completed study[36] using very bulky ligands. In numerous studies, the ΛHT2 conformer was not found for any LPt(d(G*pG*)) adduct under normal low pH to neutral conditions for all cases for which L was large enough to slow conformer interchange on the NMR time scale.[22,36,42,44,52,53] These observations led us to hypothesize that the elusive LPt(d(G*pG*)) ΛHT2 conformer (Figure 1) has a large spatial footprint, and this conformer is disfavored by carrier-ligand−G* base repulsive interactions even when L has only moderate steric bulk. Our specific goal in the present study was to employ a Goldilocks ligand that is large enough to limit the rate of dynamic motion but small enough to provide a gauge of the effects of small carrier ligands.

Steric factors influencing conformer stability include base−base, base−backbone, and base−carrier-ligand interactions. Base−base interactions are unfavorable in the HH conformation because the guanine O6 groups project toward each other and the base dipoles are aligned unfavorably, positive to positive and negative to negative.[55] In the presence of a backbone and with small carrier ligands, the prevalence of the HH1 conformer[44,62,68] suggests that unfavorable HH base−base steric and dipole interactions are relatively offset by more favorable backbone−base interactions in the HH1 conformer than in an HT conformer.

Base−base and base−ligand interactions are best assessed in the absence of a backbone, as is the case for LPt**G**$_2$ models with L bulk sufficient to slow rotation about the Pt−N7 bond of the unlinked **G**'s and hence to slow exchange between conformers. Despite the unfavorable base−base interactions, the HH conformer can form in simple LPt**G**$_2$ adducts when L has moderate bulk.[45,56,58,59,66,69] However, stronger base−base and base−carrier-ligand repulsive interactions in the HH conformer with increasing L bulk lead to a higher abundance of HT conformers of LPt**G**$_2$ adducts.[39,55,56] In the earliest NMR study on LPt**G**$_2$ adducts with a very bulky L (*N,N,N′,N′*-tetramethyldiamine), no HH conformer was found.[70] This finding was confirmed in several studies with *N,N,N′,N′*-tetramethyldiamine carrier ligands.[54,71−73] Complementing this work, as discussed in the Introduction, the (R_4dt)Pt(5′-GMP)$_2$ adducts (R = Me or Et, Figure 2) have a high abundance of the HH conformer. The high abundance is attributable to overall low steric bulk of the R_4dt ligands, allowing enough space for the HH conformer to exist without significant clashes between the O6 atoms of the 5′-GMP's.[57]

Using a strategy complementary to that employed in the present work, we have recently been examining LPt(d(G*pG*)) adducts with very bulky *N,N,N′,N′*-tetramethyl-2,3-diaminobutane (Me_4DAB) ligands with both chelate ring carbons having either the *R* or the *S* configuration. In concert with studies of LPt**G**$_2$ adducts showing that large L bulk favors HT conformers, the abundance of the ΔHT1 conformer in the Me_4DABPt(d(G*pG*)) adducts was high, reaching 66% (Table 2).[36] However, even for the Me_4DABPt(d(G*pG*)) adducts, no ΛHT2 conformer was detected except under high pH conditions, where N1H deprotonation increases dipole−dipole interactions, favoring the HT orientation of bases.

The N−Me groups in the Me_4DABPt(d(G*pG*)) adducts project above and below the coordination plane and prevent any significant degree of base canting. Canting is one structural feature whereby the H8 of a given G* base can be close to the cis G* base, and as a consequence, the H8 signal of the given G* base can be shifted upfield by the ring current anisotropy of the

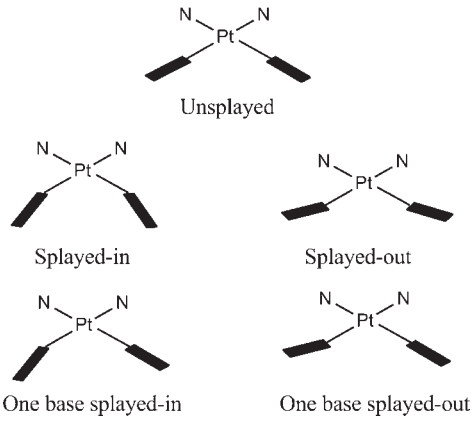

Figure 9. Depiction of different possibilities for G* base splaying in LPt(d(G*pG*)) models. The Pt and carrier ligand (not shown except for N-donor atoms) are to the rear; filled rectangles represent the G* bases.

cis G* base.[36,44,51,52,54] Even in (*R*,*R*)- and (*S*,*S*)-Me_4DABPt(d(G*pG*)), the relatively upfield H8 shifts characteristic of the ΔHT1 conformer were very similar to the corresponding H8 shifts found for adducts in which L of moderate bulk have NH groups known to facilitate canting.[36] Indeed, the upfield shifts of the two H8 signals of each conformer were identical for the two adducts, (*R*,*R*)- and (*S*,*S*)-Me_4DABPt(d(G*pG*)), providing evidence that even in cases of bulky L with N−Me groups, carrier-ligand steric effects do not influence the structure or canting of the ΔHT1 conformer. This recent study establishes that canting cannot explain the upfield H8 shifts characteristic of the ΔHT1 conformer found for all Pt(d(G*pG*)) adducts examined thus far.[36] Rather, the upfield H8 shifts were attributed to a distortion within the backbone, which brings the two uncanted G* bases into mutual close proximity. (Below, we consider the splaying-in of the G* bases in the ΔHT1 conformer.) The unusual ^{13}C NMR shifts[36] and the characteristic but unusual upfield shift of the ^{31}P NMR signal[22,36,42,44,52,53] of the ΔHT1 conformer of all LPt(d(G*pG*)) adducts provide strong evidence for a backbone distortion.

In both the DNA cross-link and the LPt(d(G*pG*)) models, the adjacent G* bases must be unstacked because the Pt−N7 bonds are nearly perpendicular to each other and form an acute angle with the plane of the base.[37,38,40] The positioning of these bases is influenced by the large 17-membered macrocyclic chelate ring created by the cross-linking. The ring could exist in a range of conformer-dependent distorted structures, with torsion angles and bond angles dependent on the conformer. Distortions could involve displacement of the Pt out of the guanine base planes, leading to splaying, wherein the bases are farther apart but the N7−N7 nonbonded and Pt−N bond distances are normal (2.9 and 2.0 Å, respectively).[37] Various possibilities for splaying are shown schematically in Figure 9. However, at least for the HH1 conformation (the only conformation for which X-ray data are available), there is evidence both for significant splaying-in[74] and for relatively little splaying-in.[37,38,40,75] Splaying-in results in the O6−O6 clashes being reduced.

In our previous LPt(d(G*pG*)) studies, we concluded that the sugar−phosphodiester backbone structure in a given conformer type does not respond appreciably to L bulk.[22,36,42,44,53] A 5′-G* N-sugar pucker and a 3′-G* S-sugar pucker were found for all the conformers of (R_4dt)Pt(d(G*pG*)) (R = Me and Et) and also for all conformers of (Me_4DAB)Pt(d(G*pG*)),[36] (5,5′-Me_2bipy)Pt(d(G*pG*)),[22] (Me_2ppz)Pt(d(G*pG*)),[53] and BipPt(d(G*pG*)).[42,44,52] Such findings are consistent with a similar structure for the sugar−phosphodiester backbone of a given conformer in all adducts. This conclusion is supported by the similarity in the shifts of the sugar proton signals and the structure-sensitive ^{31}P NMR signal of the commonly observed HH1, HH2, and ΔHT1 conformers of (R_4dt)Pt(d(G*pG*)) to those of other LPt(d(G*pG*)) adducts.[53] The new results with (R_4dt)Pt(d(G*pG*)), having a L with relatively low Goldilocks bulk near the cis G*'s, confirm and extend past findings that the backbone structures for the three now well-known conformers (HH1, HH2, ΔHT1) are similar and not sensitive to L bulk. The backbone is far from the carrier ligand, and thus, the lack of dependence of backbone structure on L appears to be reasonable. One consequence of the similar backbone structure is that the C1′-to-C1′ distances for a given conformer are similar and independent of L.

Although L bulk does not appear to influence the backbone structure, stronger G* base clashes with L as L bulk increases do introduce small but sufficient energy penalties that influence base canting and conformer distribution. The shift and intensity of NMR signals can be accurately measured, allowing detection of even small changes in canting and distribution. Before discussing distribution in detail, we consider briefly the canting of adducts in Table 2. NMR data provide evidence for base canting only in the cases of the BipPt(d(G*pG*)) adducts, in which the carrier ligand has NH groups. In such cases, the HH conformers have one canted G* base. The canting is in such a direction as to allow NH-to-G* O6 H bonding.[30,42,44,52,53] For all other L examined thus far, significant canting has not been found. Canting is not likely to be an intrinsic characteristic of the G* bases in the macrocyclic ring because the Bip ligands have moderate bulk intermediate with that of other L. Rather, the unique presence of NH groups indicates that H bonding of the O6 to an NH group is needed for significant canting. Such NH binding very likely is the reason that BipPt(d(G*pG*)) adducts form only two abundant conformers, whereas an equilibrium mixture of at least three conformers is most common in LPt(d(G*pG*)) adducts with L lacking NH groups.[42,44,52,53]

The very fact that two to three conformers of LPt(d(G*pG*)) adducts have been detected at equilibrium in every study in which the Pt−N7 rotation rate has been slowed by L bulk[22,36,42,44,52,53,72] indicates that the free energy difference between conformers is small. It is thus not surprising that changes in L bulk that modulate interactions of the carrier ligand with the G* base have enough influence to alter the distribution detectably. Even small differences of 0.1 kcal mol^{-1} in relative stability of conformers caused by differences in L−G* base steric interactions will lead to detectable differences in distribution as L is changed. Such energy differences in steric interactions are not large enough to significantly change the bond angles and most torsion angles within the macrocycle.

Above, we noted that recent work suggests that the ΔHT1 conformer has a small spatial footprint because the two bases are splayed-in.[36] This splaying-in of the bases accounts for the increase in abundance of the ΔHT1 conformer as L bulk increases because steric clashes of the carrier ligand with the bases are reduced when the bases are positioned close to each other. In contrast, because low L bulk favors the ΛHT2 conformer, we propose that both bases (or possibly only one) in the ΛHT2 conformer are splayed-out.

Before discussing the relationship of this splaying-out to ΛHT2 conformer stability, we first discuss spectral data consistent with

this proposal. Splaying-out separates the bases sufficiently to reduce H8 shielding by the cis base anisotropy, and thereby splaying-out accounts for the up to ~0.7 ppm downfield position of the ΛHT2 H8 signals compared to those of the ΔHT1 conformer. In addition, splaying-out of the bases in the ΛHT2 conformer could position the two deoxyribose C1′ atoms far enough apart to allow enough space for an undistorted backbone. Such an unstrained sugar−phosphodiester backbone conformation would explain the ~−4 ppm shift position of the ^{31}P NMR signal; this is the normal shift of an undistorted phosphodiester backbone.[76]

Splaying-out of G* bases in the ΛHT2 conformer affords a rationale for the dependence of conformer abundance on L bulk. A splayed-out base will have relatively large clashes with L. As L bulk increases, the amount of the LPt(d(G*pG*)) ΛHT2 conformer should decrease because the unfavorable base−carrier-ligand clashes will become larger. Indeed, the data in Table 2 support this relationship. Other results, in addition to the previous failure to detect any such abundant ΛHT2 conformer, support this viewpoint. In particular, the amount of the ΛHT2 conformer observed was considerably more for R = Me (40%) than for R = Et (17%) in (R_4dt)Pt(d(G*pG*)) adducts. This relatively small increase in bulk at the 6/6′ positions from Me to Et halves the abundance of the ΛHT2 conformer. Our conclusion that steric factors influence the distribution of the (Et_4dt)Pt(d(G*pG*)) conformers is supported by the presence of comparably sized NOE cross-peaks between the 3′-G* H8 and the Et_4dt methyl peaks (Figure S1, Supporting Information); these peaks indicate that the 3′-G* base is close to the cis ethyl substituent at the 6 position.

Such a marked dependence on bulk explains why the use of a relatively nonbulky L allowed us to obtain the first evidence for a fourth abundant conformer of an LPt(d(G*pG*)) adduct in its normal protonation state. It is striking that the ΛHT2 conformer for (Me_4dt)Pt(d(G*pG*)), which has a relatively small carrier ligand, is as abundant as the HH1 conformer at equilibrium (Table 2). On the other hand, the amount of the ΔHT1 conformer is expected to decrease because, when the carrier ligand is small, the unfavorable energetics of the distorted backbone conformation of the ΔHT1 conformer will not be offset by the favorable energetics of smaller base−carrier-ligand clashes characteristic of this conformer with its splayed-in bases. Thus, the (R_4dt)Pt(d(G*pG*)) adducts have the lowest abundance of the ΔHT1 conformer of any adduct, except the (*R,S,S,R*)-BipPt(d(G*pG*)) adduct, in which the NH groups are positioned to favor the HH conformers through hydrogen-bonding interactions.[42,44]

If the ΛHT2 conformer follows the pattern found for other conformers, the backbone structure of this conformer does not depend on L. Thus, for LPt(d(G*pG*)) adducts with carrier ligands of moderate or large bulk, a ΛHT2 conformer would have splayed-out bases, causing energetically unfavorable clashes with L and explaining the failure to observe this fourth conformer until now. The ΛHT2 conformer for (Me_4dt)Pt(d(G*pG*)) adducts has both G* residues in the anti conformation. In one previous case, in which a fourth conformer could be examined by NMR methods, one residue was syn.[36] However, in that case the conformer existed only at high pH, where the bases are deprotonated.[36]

Another noteworthy feature of the distributions given in Table 2 is the finding that the HH1 conformer generally has relatively high abundance. However, its abundance is lowest both with a large carrier ligand (Me_4DAB) and with a small carrier ligand (Me_4dt). Likewise, there is no clear trend in the HH1 to HH2 ratio. Clearly then, in addition to overall apparent bulk, the shape of the carrier ligand relative to the structure of the macrocyclic ring moiety has a secondary effect on relative conformer stability.

Factors Influencing Interchange Rates. For both LPt(d(G*pG*)) and LPt$\mathbf{G}_2$ intrastrand cross-link models, interchange rates depend on the severity of steric clashes between the guanine base and L as the base rotates around the Pt−N7 bond because base rotation decreases the distance between the guanine O6 and L. Conformational changes (involving the backbone and in some cases the glycosidic bond) that must accompany base rotation in linked models require energy and could increase the activation barrier for an LPt(d(G*pG*)) adduct vs the corresponding LPt$\mathbf{G}_2$ adduct. Thus, one might expect that the macrocyclic ring would decrease the conformer interchange rate relative to that of the unlinked analogues. However, the activation barrier (and hence the reaction rate) depends on the relative energies of the ground and transition states. Thus, if the macrocyclic ring destabilizes the ground state relative to the transition state (for example, by restricting the bases to unfavorable positions in the ground state, preventing optimal overlap between the N7 lone pair and the Pt $d_{x^2-y^2}$ orbital), the activation barrier would be decreased. Thus, conformer interchange could be more rapid in a linked LPt(d(G*pG*)) model than in the equivalent unlinked LPt$\mathbf{G}_2$ model with the same L. Consequently, the effect of the backbone on the rate of conformer interconversion cannot be predicted.

In the past, suitable L's were not available to provide a convenient comparison of relative interchange rates. Comparison of the linked and unlinked (R_4dt)Pt models leaves little doubt that the backbone greatly slows the interchange rate. Interchange of conformers of the (R_4dt)Pt(d(G*pG*)) adducts took days, whereas we observed EXSY peaks for the (R_4dt)Pt(5′-GMP)$_2$ models (interchange of the order of seconds or less). The conformers of the LPt(5′-GMP)$_2$ adducts typically interchange more slowly than LPt$\mathbf{G}_2$ adducts with other **G**'s.[55] The (R_4dt)Pt models thus provide a clear and striking case that, at least for a Goldilocks L, the presence of the sugar−phosphodiester backbone dramatically decreases the interchange rate.

The rate at which the ΛHT2 conformer of (Me_4dt)Pt(d(G*pG*)) forms from other conformers is remarkably low, as revealed by NMR results described above. If, as we surmise, one or both bases are particularly splayed-out in the ΛHT2 conformer, then base rotation around the Pt−N7 bond would lead to severe clashes of the base with L in the transition state, raising the activation barrier. Thus, the rate of base rotation required for the ΛHT2 conformer to form or to convert to another conformer would be expected to be slow, as found. From the law of microscopic reversibility, the high abundance of the ΛHT2 conformer (Table 2) requires that the ΛHT2 conformer converts to give the other (and known) conformers relatively slowly, as confirmed by HPLC data described above.

■ CONCLUSIONS

We conclude that backbone strain and base−base, base−ligand, and base−backbone interactions all contribute to determining the relative stability of the conformers of LPt(d(G*pG*)) adducts. These factors also influence the rate of interchange between these conformers.

The base−base and base−ligand interactions are well understood from the unlinked LPt$\mathbf{G}_2$ adducts.[7,45,55,57,65,77,78] Our new

results provide clarification of the importance of the base−backbone interactions and backbone strain. For the well-known conformers, HH1, HH2, and ΔHT1, all results have pointed to a relative invariance of the backbone structure for a given conformer independent of the carrier ligand. The R_4dt ligands used in the present study are less bulky than those previously used. The backbone structure of a given conformer in the (R_4dt)Pt(d(G*pG*)) adducts is nevertheless similar to that of the respective conformer in LPt(d(G*pG*)) adducts with bulkier carrier ligands. We conclude that steric interactions of L with the d(G*pG*) moiety are not strong enough to influence backbone structure and that the structure does not change even when L has low bulk.

Because an HT arrangement is best for minimizing base−base repulsive interactions, the prevalence of HH conformers in LPt(d(G*pG*)) adducts suggests clearly that the backbone disfavors the ΔHT1 conformer. The increased amount of the ΔHT1 conformer as the carrier-ligand bulk increases parallels the finding in unlinked adducts that bulk favors HT over HH conformers, a finding attributable to lower steric repulsion between the bases and to more favorable dipole−dipole interactions in the HT versus the HH orientation.[36,45,59] For the ΔHT1 conformer, favorable decreases in base−ligand repulsions may outweigh the unfavorable base−backbone repulsions and backbone strain for this conformer. However, because R_4dt carrier ligands have low bulk, base−ligand repulsions are less important in influencing the relative stability of conformers of (R_4dt)Pt(d(G*pG*)) adducts. Consequently, these adducts have the lowest abundance of the ΔHT1 conformer yet observed.

For the HH conformers, the more favorable base−backbone interactions and the possibly lower backbone strain appear to largely offset the less favorable base−base and base−ligand steric interactions for HH conformers. Consequently, HH conformers are found to be abundant for all adducts regardless of carrier-ligand bulk.

For the ΛHT2 conformer, the favorable aspects of an HT orientation may be outweighed by the unfavorable base−backbone repulsions for this conformer in adducts having carrier ligands of moderate to high bulk; these repulsions are expected to keep the bases splayed-out, resulting in unfavorable base−ligand repulsions. When the carrier ligand is small, the bases have space to splay out and the ΛHT2 conformer becomes more stable. In addition, the backbone is less strained; the lower strain contributes to the stability of the conformer. The ΛHT2 conformer of the (Me_4dt)Pt(d(G*pG*)) adduct has a high abundance because of the small size of the carrier ligand. The slightly greater bulk of the Et_4dt carrier ligand explains why the ΛHT2 conformer of the (Et_4dt)Pt(d(G*pG*)) adduct has one-half the abundance of the ΛHT2 conformer of the (Me_4dt)Pt(d(G*pG*)) adduct.

The ΛHT2 conformer of (R_4dt)Pt(d(G*pG*)) adducts becomes abundant slowly. The increase in base−ligand repulsions accompanying base rotation as other conformers convert to this ΛHT2 conformer is greater compared to increases in these repulsions as the HH1, HH2, and ΔHT1 conformers interconvert. The absence of any EXSY cross-peaks for the (R_4dt)Pt(d(G*pG*)) adduct and the presence of such cross-peaks for the (R_4dt)Pt(5′-GMP)$_2$ adduct[57] provide the first clear evidence that the sugar−phosphodiester backbone between two adjacent G*'s in LPt(d(G*pG*)) adducts slows conformer interchange relative to the rapidity of this process in the corresponding LPt**G**$_2$ adducts.

Canting is likely to be an integral component of the structural distortion in DNA responsible for the anticancer activity. The new results indicate that the base canting present in adducts derived from active anticancer drugs, which for the cis bifunctional agents have carrier ligands with NH groups, is not an intrinsic property of the Pt(d(G*pG*)) macrocycle. Rather, it seems likely that the hydrogen bonding involving the NH groups facilitates the canting found in those X-ray structures most relevant to distortions in DNA caused by the most active anticancer drugs.[37,38,40,74,75]

■ ASSOCIATED CONTENT

Supporting Information. ROESY spectrum showing G* H8-to-sugar and G* H8-to-methyl ^{1}H−^{1}H NOE cross-peaks for the (Et_4dt)Pt(d(G*pG*)) adduct, as well as a discussion analyzing the NMR and HPLC data for this adduct; 1D ^{1}H NMR and ROESY spectra of a (Me_4dt)Pt(d(G*pG*)) sample having a large abundance of the ΛHT2 conformer; HPLC chromatograms of (Me_4dt)Pt(d(G*pG*)) fractions collected at different retention times upon reinjection after 1 day and after 4 days; discussion of possible pathways responsible for the interconversion of conformers. This material is available free of charge via the Internet at http://pubs.acs.org.

■ AUTHOR INFORMATION

Corresponding Author
*E-mail: lmarzil@lsu.edu.

■ ACKNOWLEDGMENT

Instrumentation used in this study was supported by NSF Grant No. 0421356. We thank Thomas Weldeghiorghis for his help in obtaining some of the ROESY spectra on the Varian spectrometer (700 MHz).

■ REFERENCES

(1) Kelland, L. *Nature (London)* **2007**, *7*, 573–584.
(2) Arnesano, F.; Natile, G. *Coord. Chem. Rev.* **2009**, *253*, 2070–2081.
(3) Klein, A. V.; Hambley, T. W. *Chem. Rev.* **2009**, *109*, 4911–4920.
(4) Reedijk, J. *Eur. J. Inorg. Chem.* **2009**, *2009*, 1303–1312.
(5) Jakupec, M. A.; Galanski, M.; Arion, V. B.; Hartinger, C. G.; Keppler, B. K. *Dalton Trans.* **2008**, 183–194.
(6) Mier-Vinué, J. D.; Gay, M.; Montaña, A. M.; Sáez, R.-I.; Moreno, V.; Kasparkova, J.; Vrana, O.; Heringova, P.; Brabec, V.; Boccarelli, A.; Coluccia, M.; Natile, G. *J. Med. Chem.* **2008**, *51*, 424–431.
(7) Intini, F. P.; Cini, R.; Tamasi, G.; Hursthouse, M. B.; Natile, G. *Inorg. Chem.* **2008**, *47*, 4909–4917.
(8) Lovejoy, K. S.; Todd, R. C.; Zhang, S.; McCormick, M. S.; D'Auino, J. A.; Reardon, J. T.; Sancar, A.; Giacomini, K. M.; Lippard, S. J. *Proc. Natl. Acad. Sci. U.S.A.* **2008**, *105*, 8902–8907.
(9) Ober, M.; Lippard, S. J. *J. Am. Chem. Soc.* **2008**, *130*, 2851–2861.
(10) Arnesano, F.; Natile, G. *Pure Appl. Chem.* **2008**, *80*, 2715–2725.
(11) Todd, R. C.; Lippard, S. J. *Metallomics* **2009**, *1*, 280–291.
(12) Dolfen, D.; Schottler, K.; Valiahdi, S.-M.; Jakupec, M. A.; Keppler, B. K.; Tiekink, E. R. T.; Mohr, F. *J. Inorg. Biochem.* **2008**, *102*, 2067–2071.
(13) Mitchell, C.; Kabolizadeh, P.; Ryan, J.; Roberts, J. D.; Yacoub, A.; Curiel, D. T.; Fisher, P. B.; Hagan, M. P.; Farrell, N. P.; Grant, S.; Dent, P. *Mol. Pharmacol.* **2007**, *72*, 704–714.
(14) Billecke, C.; Finniss, S.; Tahash, L.; Miller, C.; Mikkelsen, T.; Farrell, N. P.; Bogler, O. *Neuro-Oncology* **2006**, *8*, 215–226.
(15) Teletchea, S.; Komeda, S.; Teuben, J.-M.; Elizondo-Riojas, M.-A.; Reedijk, J.; Kozelka, J. *Chem.—Eur. J.* **2006**, *12*, 3741–3753.

(16) Ma, Z.; Choudhury, J. R.; Wright, M. W.; Day, C. S.; Saluta, G.; Kucera, G. L.; Bierbach, U. *J. Med. Chem.* **2008**, *51*, 7574–7580.
(17) Ma, Z.; Saluta, G.; Kucera, G. L.; Bierbach, U. *Bioorg. Med. Chem. Lett.* **2008**, *18*, 3799–3801.
(18) Aris, S. M.; Farrell, N. P. *Eur. J. Inorg. Chem.* **2009**, *2009*, 1293–1302.
(19) Krause-Heuer, A. M.; Grünert, R.; Kühne, S.; Buczkowska, M.; Wheate, N. J.; Le Pevelen, D.; Boag, L. R.; Fisher, D. M.; Kasparkova, J.; Malina, J.; Bednarski, P. J.; Brabec, V.; Aldrich-Wright, J. R. *J. Med. Chem.* **2009**, *52*, 5474–5484.
(20) Beljanski, V.; Villanueva, J. M.; Doetsch, P. W.; Natile, G.; Marzilli, L. G. *J. Am. Chem. Soc.* **2005**, *127*, 15833–15842.
(21) Marzilli, L. G.; Saad, J. S.; Kuklenyik, Z.; Keating, K. A.; Xu, Y. *J. Am. Chem. Soc.* **2001**, *123*, 2764–2770.
(22) Bhattacharyya, D.; Marzilli, P. A.; Marzilli, L. G. *Inorg. Chem.* **2005**, *44*, 7644–7651.
(23) Kasparkova, J.; Vojtiskova, M.; Natile, G.; Brabec, V. *Chem.—Eur. J.* **2008**, *14*, 1330–1341.
(24) Malina, J.; Novakava, O.; Vojtiskova, M.; Natile, G.; Brabec, V. *Biophys. Chem.* **2007**, *93*, 3950–3962.
(25) Hambley, T. W. *Coord. Chem. Rev.* **1997**, *166*, 181–223.
(26) Orbell, J. D.; Taylor, M. R.; Birch, S. L.; Lawton, S. E.; Vilkins, L. M.; Keefe, L. J. *Inorg. Chim. Acta* **1988**, *152*, 125–134.
(27) Benedetti, M.; Malina, J.; Kaspárková, J.; Brabec, V.; Natile, G. *Environ. Health Perspect.* **2002**, *110*, 779–782.
(28) Hirano, T.; Inagaki, K.; Fukai, T.; Alink, M.; Nakahara, H.; Kidani, Y. *Chem. Pharm. Bull.* **1990**, *38*, 2850–2852.
(29) Todd, R. C.; Lippard, S. J. In *Platinum and Other Heavy Metal Compounds in Cancer Chemotherapy*; Bonetti, A., Leone, R., Muggia, F. M., Howell, S. B., Eds.; Humana Press: Totowa, NJ, 2009; pp 67−72.
(30) Saad, J. S.; Natile, G.; Marzilli, L. G. *J. Am. Chem. Soc.* **2009**, *131*, 12314–12324.
(31) Coluccia, M.; Nassi, A.; Loseto, F.; Boccarelli, A.; Mariggio, M. A.; Giordano, D.; Intini, F. P.; Caputo, P.; Natile, G. *J. Med. Chem.* **1993**, *36*, 510–512.
(32) Coluccia, M.; Natile, G. *Anti-Cancer Agents Med. Chem.* **2007**, *7*, 111–123.
(33) Alvheim, C.; Frøystein, N. A.; Vinje, J.; Intini, F. P.; Natile, G.; Liu, Y.; Huang, R.; Sletten, E. *Inorg. Chim. Acta* **2009**, *362*, 907–914.
(34) Intini, F. P.; Pellicani, R. Z.; Bccarelli, A.; Sasanelli, R.; Coluccia, M.; Natile, G. *Eur. J. Inorg. Chem.* **2008**, *2008*, 4555–4561.
(35) Halámiková, A.; Heringová, P.; Kašpárková, J.; Intini, F. P.; Natile, G.; Nemirovski, A.; Gibson, D.; Brabec, V. *J. Inorg. Biochem.* **2008**, *102*, 1077–1089.
(36) Saad, J. S.; Benedetti, M.; Natile, G.; Marzilli, L. G. *Inorg. Chem.* **2011**, *50*, 4559–4571.
(37) Sherman, S. E.; Gibson, D.; Wang, A.; Lippard, S. J. *J. Am. Chem. Soc.* **1988**, *110*, 7368–7381.
(38) Sherman, S. E.; Gibson, D.; Wang, A. H.-J.; Lippard, S. J. *Science (Washington, D. C.)* **1985**, *230*, 412–417.
(39) Ano, S. O.; Kuklenyik, Z.; Marzilli, L. G. In *Cisplatin. Chemistry and Biochemistry of a Leading Anticancer Drug*; Lippert, B., Ed.; Wiley-VCH: Weinheim, 1999; pp 247−291.
(40) Ohndorf, U.-M.; Rould, M. A.; He, Q.; Pabo, C. O.; Lippard, S. J. *Nature (London)* **1999**, *399*, 708–712.
(41) Sullivan, S. T.; Saad, J. S.; Fanizzi, F. P.; Marzilli, L. G. *J. Am. Chem. Soc.* **2002**, *124*, 1558–1559.
(42) Williams, K. M.; Cerasino, L.; Natile, G.; Marzilli, L. G. *J. Am. Chem. Soc.* **2000**, *122*, 8021–8030.
(43) Williams, K. M.; Scarcia, T.; Natile, G.; Marzilli, L. G. *Inorg. Chem.* **2001**, *40*, 445–454.
(44) Ano, S. O.; Intini, F. P.; Natile, G.; Marzilli, L. G. *J. Am. Chem. Soc.* **1998**, *120*, 12017–12022.
(45) Saad, J. S.; Scarcia, T.; Shinozuka, K.; Natile, G.; Marzilli, L. G. *Inorg. Chem.* **2002**, *41*, 546–557.
(46) Sherman, S. E.; Lippard, S. J. *Chem. Rev.* **1987**, *87*, 1153–1181.
(47) den Hartog, J. H. J.; Altona, C.; Chottard, J.-C.; Girault, J.-P.; Lallemand, J.-Y.; de Leeuw, F. A.; Marcelis, A. T. M.; Reedijk, J. *Nucleic Acids Res.* **1982**, *21*, 1352–1356.
(48) Girault, J.-P.; Chottard, G.; Lallemand, J.-Y.; Chottard, J.-C. *Biochemistry* **1982**, *21*, 1352–1356.
(49) Yang, D.; van Boom, S.; Reedijk, J.; van Boom, J.; Wang, A. *Biochemistry* **1995**, *34*, 12912–12920.
(50) Chottard, J.-C.; Girault, J.-P.; Chottard, G.; Lallemand, J.-Y.; Mansuy, D. *J. Am. Chem. Soc.* **1980**, *102*, 5565–5572.
(51) Kozelka, J.; Fouchet, M. H.; Chottard, J.-C. *Eur. J. Biochem.* **1992**, *205*, 895–906.
(52) Marzilli, L. G.; Ano, S. O.; Intini, F. P.; Natile, G. *J. Am. Chem. Soc.* **1999**, *121*, 9133–9142.
(53) Sullivan, S. T.; Ciccarese, A.; Fanizzi, F. P.; Marzilli, L. G. *J. Am. Chem. Soc.* **2001**, *123*, 9345–9355.
(54) Saad, J. S.; Benedetti, M.; Natile, G.; Marzilli, L. G. *Inorg. Chem.* **2010**, *49*, 5573–5583.
(55) Natile, G.; Marzilli, L. G. *Coord. Chem. Rev.* **2006**, *250*, 1315–1331.
(56) Ano, S. O.; Intini, F. P.; Natile, G.; Marzilli, L. G. *J. Am. Chem. Soc.* **1997**, *119*, 8570–8571.
(57) Maheshwari, V.; Marzilli, P. A.; Marzilli, L. G. *Inorg. Chem.* **2008**, *47*, 9303–9313.
(58) Ano, S. O.; Intini, F. P.; Natile, G.; Marzilli, L. G. *Inorg. Chem.* **1999**, *38*, 2989–2999.
(59) Saad, J. S.; Scarcia, T.; Natile, G.; Marzilli, L. G. *Inorg. Chem.* **2002**, *41*, 4923–4935.
(60) Williams, K. M.; Cerasino, L.; Intini, F. P.; Natile, G.; Marzilli, L. G. *Inorg. Chem.* **1998**, *37*, 5260–5268.
(61) Intini, F. P.; Cini, R.; Tamasi, G.; Hursthouse, M. B.; Marzilli, L. G.; Natile, G. *Inorg. Chem.* **2010**, *49*, 7853–7860.
(62) Berners-Price, S. J.; Ranford, J. D.; Sadler, P. J. *Inorg. Chem.* **1994**, *33*, 584–5846.
(63) den Hartog, J. H. J.; Altona, C.; van der Marel, G. A.; Reedijk, J. *Eur. J. Biochem.* **1985**, *147*, 371–379.
(64) Mukundan, S., Jr.; Xu, Y.; Zon, G.; Marzilli, L. G. *J. Am. Chem. Soc.* **1991**, *113*, 3021–3027.
(65) Sullivan, S. T.; Ciccarese, A.; Fanizzi, F. P.; Marzilli, L. G. *Inorg. Chem.* **2000**, *39*, 836–842.
(66) Marzilli, L. G.; Intini, F. P.; Kiser, D.; Wong, H. C.; Ano, S. O.; Marzilli, P. A.; Natile, G. *Inorg. Chem.* **1998**, *37*, 6898–6905.
(67) Benedetti, M.; Marzilli, L. G.; Natile, G. *Chem.—Eur. J.* **2005**, *11*, 5302–5310.
(68) Neumann, J.-M.; Tran-Dinh, S.; Girault, J.-P.; Chottard, J.-C.; Huynh-Dinh, T. *Eur. J. Biochem.* **1984**, *141*, 465–472.
(69) Xu, Y.; Natile, G.; Intini, F. P.; Marzilli, L. G. *J. Am. Chem. Soc.* **1990**, *112*, 8177–8179.
(70) Cramer, R. E.; Dahlstrom, P. L. *J. Am. Chem. Soc.* **1979**, *101*, 3679–3681.
(71) Benedetti, M.; Gabriella, T.; Cini, R.; Marzilli, L. G.; Natile, G. *Chem.—Eur. J.* **2007**, *13*, 3131–3142.
(72) Benedetti, M.; Saad, J. S.; Marzilli, L. G.; Natile, G. *Dalton Trans* **2003**, *5*, 872–879.
(73) Benedetti, M.; Tamasi, G.; Cini, R.; Natile, G. *Chem.—Eur. J.* **2003**, *9*, 6122–6132.
(74) Spingler, B.; Whittington, D. A.; Lippard, S. J. *Inorg. Chem.* **2001**, *40*, 5596–5602.
(75) Admiraal, G.; van der Veer, J. L.; de Graaff, R. A. G.; den Hartog, J. H. J.; Reedijk, J. *J. Am. Chem. Soc.* **1987**, *109*, 592–594.
(76) Byrd, R. A.; Summers, M. F.; Zon, G.; Fouts, C. S.; Marzilli, L. G. *J. Am. Chem. Soc.* **1986**, *108*, 504–505.
(77) Wong, H. C.; Shinozuka, K.; Natile, G.; Marzilli, L. G. *Inorg. Chim. Acta* **2000**, *297*, 36–46.
(78) Sullivan, S. T.; Ciccarese, A.; Fanizzi, F. P.; Marzilli, L. G. *Inorg. Chem.* **2001**, *40*, 455–462.